

Watt-level ultrafast 1.75 μm laser system based on thulium-doped core and terbium-doped cladding fluoride fibers

Dina Grace Banguilan¹, Yuto Iye¹, Kazuhiko Ogawa²,
Eiji Kajikawa² and Takao Fuji¹

¹Laser Science Laboratory, Toyota Technological Institute, 2-12-1 Hisakata, Tempaku-ku, Nagoya, 468-8511, Japan

²FiberLabs Inc., KDDI Laboratories Building, 2-1-15 Ohara, Fujimino, Saitama 356-8502, Japan

E-mail: dcbanguilan@toyota-ti.ac.jp

November 2025

Abstract. We report watt-level femtosecond pulses in the 1.75 μm region using a thulium-doped core, terbium-doped cladding fluoride (Tm:Tb:ZBLAN) fiber laser system. The seed pulse is generated through stimulated Raman scattering in a silica fiber pumped by an erbium-doped fiber laser. The soliton is subsequently amplified through a multi-stage Tm:Tb:ZBLAN amplifier. The tunability of our chirped fiber Bragg grating stretcher, matched with a Treacy compressor, compresses the pulse to 217 fs. Our system generates \sim 250 nJ of single-pulse energy, with a corresponding average power of \sim 1 W at a 4 MHz repetition rate. The laser system is suitable for multiphoton microscopy.

1. Introduction

Fiber laser systems operating within the short-wavelength infrared region (SWIR). (1.0–2.0 μm) have attracted significant interest due to their importance in multi-photon microscopy (MPM) [1–4] and communication systems [5, 6]. In MPM, the nonlinear nature of multiphoton excitation demands high average power, and to stay within safe limits for biological tissues, requires low repetition rate. Pulse durations around 200 fs are ideal, as they enhance the probability of simultaneous multiphoton absorption events by a single fluorescent compound [7]. Therefore, developing a fiber laser system that is both simple and capable of delivering sufficient average power with reasonable pulse duration and repetition rate at 1.75 μm is highly desirable. The compact and simple design of fiber lasers is favored for easier integration in bioimaging experiments. In fluorescence-based MPM, the 1.75 μm band is preferred, as it offers a window, where the combined effects of absorption and scattering are minimized in most biological tissues [8].

However, laser development faces a challenge in identifying a suitable gain medium that can operate efficiently within the restricted SWIR and achieve direct pulse generation and amplification with the required output parameters for MPM. In Ref. [9], high-germania bismuth active fiber was able to operate in the 1.75 μm . However the pulse duration is too long (≥ 600 fs) for MPM.

Thulium-doped (Tm) fibers are well-capable of the direct generation of ultrashort pulses in the target wavelength as it exhibits a broad emission, spanning 1.6 to 2.1 μm owing to the 3F_4 to 3H_6 energy-level transition of Tm ions [10, 11]. For MPM applications, however, some ingenuity is required to mitigate the undesirable amplified spontaneous emission (ASE) at long wavelength region (≥ 1.8 μm) of the Tm emission which can damage samples in *in vivo* imaging applications. For instance, the periodic structures in photonic crystal cause interference effects, resulting in a photonic bandgap—a wavelength range that cannot propagate through the crystal. Although a wide tuning range is achieved through this scheme, the pulse duration remains in the \sim ps scale, which is not suitable for MPM [12]. Moreover, it requires advanced fabrication techniques. Chen and his group demonstrated short-pass filtering at 1.7 μm using W-type normal dispersion Tm-doped fibers [13–15]. They generated femtosecond pulses using a bend-induced wave selection technique to suppress longer wavelengths. However, their results showed pedestals that carry considerable energy. This could be attributed to strong nonlinear effects that distort the phase of ultrashort pulses during propagation through excessively long fibers in their system. That free-space components should still be considered to reduce these pedestals.

In this paper, we present a multistage ultrafast amplifier system based on Tm:Tb:ZBLAN fibers. Unlike in Ref. [12] which requires an advance fabrication process or in Ref. [15], which depends on mechanical bending for short-pass filtering effect, our technique is based on ionic codoping. We doped the cladding with Tb ions to effectively eliminate amplification in the long wavelength range. The absorption spectrum of the Tb ion is centered at ~ 1.9 μm [5]. Essentially, the Tb ions act as an energy sink for the long-wavelength photons emitted by the Tm ions. Here, we use ZBLAN glass as the host material because it has almost zero dispersion near 1.75 μm . This property can lead to high quality pulse compression. A ZBLAN fiber also has a higher efficiency compared to silica fiber when used as an active fiber because its lower phonon energy reduces non-radiative decay, leading to a longer upper-state lifetime, which is crucial for achieving sufficient gain [3, 16, 17]. In addition to this, we have also improved our compression stage by incorporating a chirped fiber Bragg grating (CFBG) on-demand paired with a Treacy grating compressor for controlled dispersion management. With these, we have succeeded in generating watt-level pulses at 1.76 μm and compressed pedestal-free pulses of 217 fs duration, which are suitable for MPM.

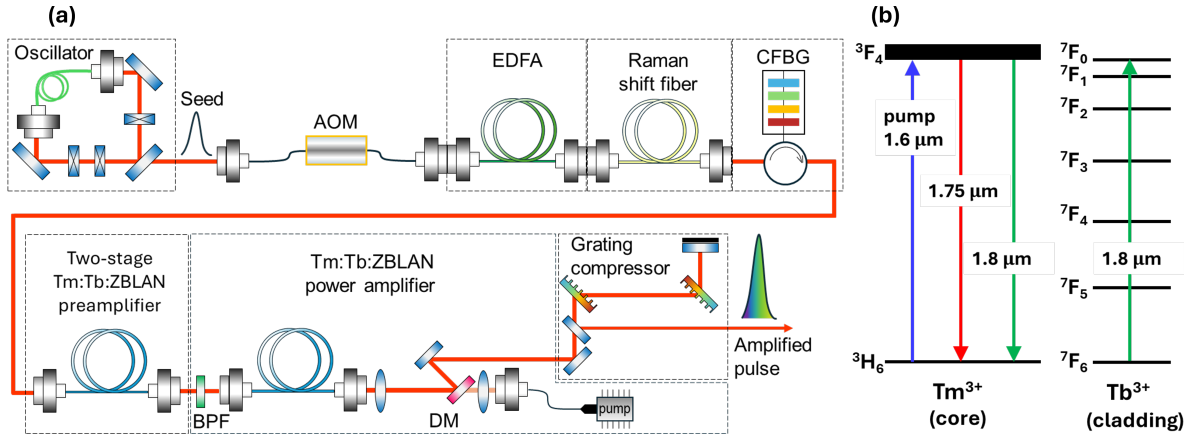


Figure 1. (a) Schematic of the laser system. AOM: acousto-optic modulator, EDFA: Erbium-doped fiber amplifier, CFBG: chirped fiber Bragg grating, BPF: bandpass filter, and DM: dichroic mirror. (b) Energy level transitions of Tm³⁺ and Tb³⁺.

2. Tm:Tb:ZBLAN laser system

Figure 1(a) shows the schematic of the laser system based on Tm:Tb:ZBLAN fibers. The system started with an Er:SiO₂ fiber laser oscillator mode-locked using nonlinear polarization rotation (FL-MLEr-kit, Kokyo). The oscillator's output was spectrally filtered to remove the Kelly's sidebands according to the technique in Ref. [18]. Initially, the pulse repetition frequency, as determined by the cavity length was 24 MHz and was reduced to 4 MHz using an acousto-optic modulator (AOM). The pulse was amplified with a home-built ultrafast Er:SiO₂ amplifier. The 1.75 μ m seed was generated through soliton self-frequency shift of the amplified 1560 nm pulses. The Raman shift fiber was a small cladding polarization-maintained silica fiber (RCHA15-PS-U17C, MFD:6.0 μ m @1550 nm, Fujikura) with a length of 5 m. Figure 2 shows the spectra from the Raman shift fiber with various pump currents. The transform limited duration of the 1.75 μ m soliton is 95 fs by assuming a sech² pulse shape. The 1.75 μ m component was estimated to be 8.7 mW. Then it was sent to a CFBG-based tunable pulse stretcher (*TPSR*, *TeraXion*) which introduces an initial group delay dispersion (GDD) and third-order dispersion (TOD) of +7.1435 ps² and -0.0585 ps³, respectively, and can be tuned. The tuning range of our CFBG is 0.0525 ps² for GDD and 0.0027 ps³ for TOD. The CFBG stretches the pulse to \sim 112 ps. The spectrum after the CFBG is slightly narrower than that of the soliton due to the diffraction bandwidth of the CFBG (see Fig. 2). The average power of the stretched pulse was estimated to be 0.35 mW. The low output power after the CFBG is due to the insertion losses of the input and output ports of the circulator in addition to the 30% reflectivity loss of the CFBG. The total loss within the CFBG and the circulator is 6.6 dB.

The stretched pulse was sent to a two-stage Tm:Tb:ZBLAN fiber preamplifier, whose output is further amplified with a power amplifier. Essentially, the direct amplification of the 1.75 μ m in our multistage amplifier system relies on the 3F_4 to 3H_6

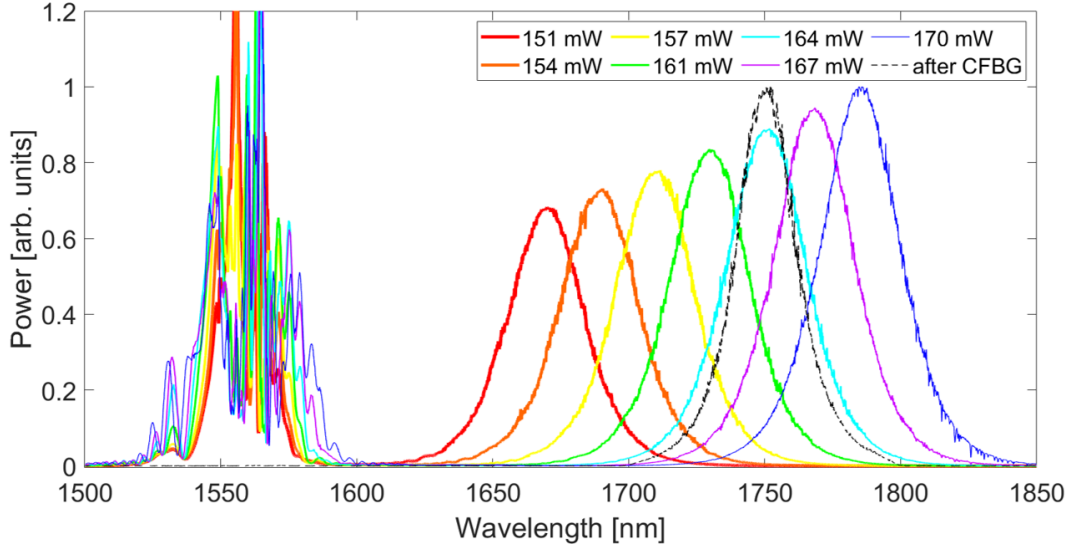


Figure 2. Output spectra of the Raman shift fiber with various pump powers for the EDFA. The pulse reflected by the CFBG is also shown.

energy-level transition of Tm ions. T. Sakamoto et al. firstly designed and fabricated a Tm–Tb-doped fiber, which had a Tm-doped fiber core and a Tb-doped fiber cladding [5]. As illustrated in Figure 1(b), the Tb-doped cladding drives the Tm^{3+} gain spectrum to the 1.75 μm region because the 1.8–2 μm ASE of Tm^{3+} is well suppressed by the ground state absorption of Tb^{3+} [11].

The first preamplification stage is based on fiber coupling. The Tm:Tb:ZBLAN fiber is pumped by a continuous wave 1600 nm Er:SiO₂ fiber laser (VFLS-1600-M-5-FA, Connet). The diameter of the core, the NA, the length, the Tm and Tb doping concentration of the fiber were 8.5 μm , 1.6 m, 0.14, 2500 ppm and 3000 ppm, respectively. The ZBLAN fiber was connected to wavelength division multiplexing (WDM) based on SMF28 silica fibers with optical contact. The losses of the input and output ports for the seed pulse were 0.8 dB and 0.9 dB, respectively. The spectra of the amplified stimulated emission with several pump powers are shown in Fig. 3(a). The average power of the amplified pulses was 12 mW with 3 W pumping at a repetition rate of 4 MHz. The slope efficiency was 0.6 % and can be improved by increasing the throughput of the CFBG. The pulse was further amplified using a second stage preamplifier after the pulse passed through a bandpass filter (BP-1693-140).

The second preamplifier consists of a Tm:Tb:ZBLAN with a core diameter of 7.5 μm , NA of 0.14, a doping concentration of 2500 ppm for Tm and 3000 ppm for Tb and a length of 3 m. While the first preamplifier is based on fiber coupling, the second stage is based on space coupling to avoid too much nonlinear effect during propagation of the amplified pulse. The pump laser is the same 1600 nm Er:SiO₂ fiber laser (VFLS-1600-B-5-FA, Connet). The output spectra of the second amplifier is shown in Fig. 3(b) until 4 W of pumping power. We did not observe an obvious change in the shape of the

amplified spectrum though it is slightly red-shifted by ~ 3 nm compared to the output of the first stage. This may be due to Tm:Tb:ZBLAN having higher gain at longer wavelengths. Nonetheless, it is very unlikely that such a very small shift affects the compression quality of the final output. The central wavelength of the spectrum peaked at 1.75 μ m which is shorter than in our previous system (1.77 μ m) [19]. The output power of the second preamplifier with 4 W pumping was 232 mW, which is almost twice higher than our previous report (130 mW) at a 4 MHz repetition rate [19]. The slope efficiency is 5.7 %. The second preamplifier improved because of the use of a longer active fiber which enhances population inversion and thus a higher gain. The noise in the long wavelength region (≥ 1.8 μ m) is also suppressed very well with almost 10³-fold power level difference to the central peak.

The power amplifier also consisted of a Tm:Tb:ZBLAN fiber with a core diameter of 7.6 μ m, a length of 4 m, and a doping concentration of 2500 ppm for Tm and 3000 ppm for Tb. The spectrum of the ASE of the active fiber with the pump power of 9.75 W is shown in black dash line in Fig. 3(c). To ensure that we only amplify the target 1.75 μ m wavelength and filter out otherwise dominant long wavelength emission (≥ 1.8 μ m), we inserted a bandpass filter (BP-1690-095) at the output of the second preamplifier. The BPF takes the function of the 4f system in our previous system but now with lesser footprint [19]. The pump laser for the power amplifier is a commercially available Raman shift fiber laser (RLR-30-1620, IPG photonics). The output spectrum of the power amplifier is shown in Fig. 3(c) for several pump powers. The ASE was suppressed well as the amplified pulse peaked around 1.76 μ m. We see some intensity in the long wavelength region (≥ 1.8 μ m) but we can easily remove it at the compression stage without losing too much power. With respect to the second preamplifier spectrum, the output spectrum is slightly shifted towards the longer wavelength region where the gain is higher. No obvious spectral broadening or narrowing was observed, indicating that nonlinear effects were well controlled during the amplification process. The pump power dependence of the output power was linear up to 4.21 W and was slightly saturated. The slope efficiency was calculated to be 13.2 % by fitting the output power up to the 4.21 W absorbed pump power. At 9.75 W pump power, the output power reached ~ 1 W. We estimated ~ 250 nJ of single pulse energy. The output power and the slope efficiency can still be improved by boosting the seed pulse. As we have observed, the gain of the Tm:Tb:ZBLAN fiber at the second stage has not reached the saturation point, implying that the output power can be further increased with higher pumping power.

Unlike in Ref. [19], we used Tm:Tb:ZBLAN fiber in the power amplifier similar to the preamplifiers to reduce the complexity of the laser system. To our knowledge, this is the first all-Tm:Tb:ZBLAN fiber system designed to directly amplify watt-level ultrafast pulses at 1.76 μ m. The peak-to-peak fluctuation measurement resulted in an rms value of 6% at 20000 counts, which was recorded with a high speed InGaAs detector and a 1 GHz digital oscilloscope. Since the amplified pulse came out from a single mode fiber, the amplified beam had an almost Gaussian profile. The polarization of the final output can be controlled by using a half-wave plate and a quarter-wave plate.

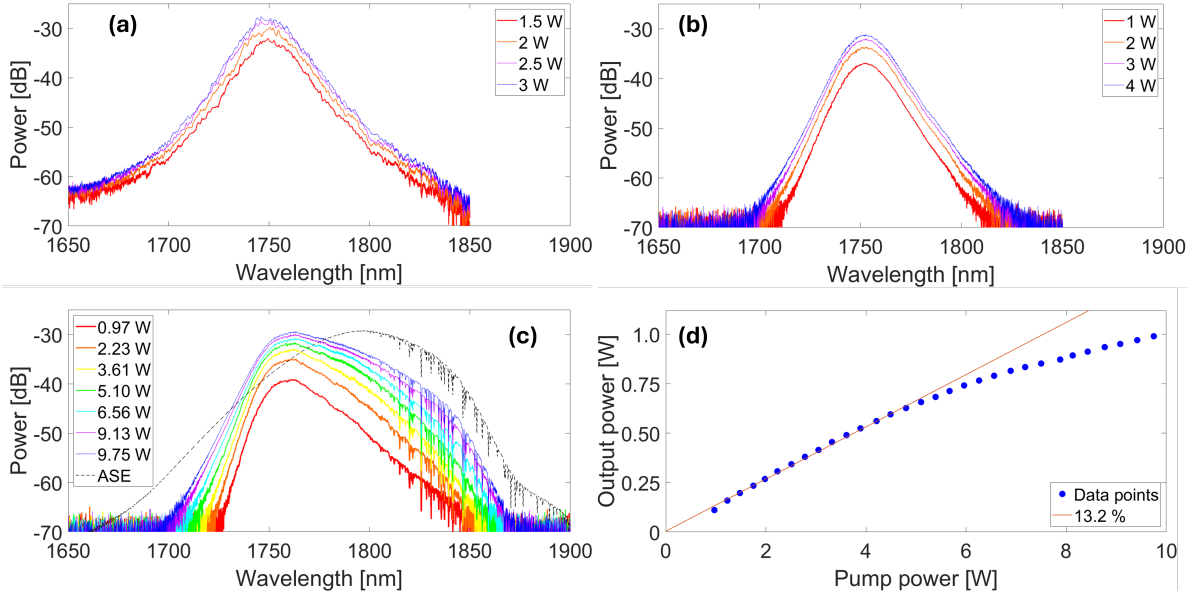


Figure 3. (a) Output spectra of the first Tm:Tb:ZBLAN preamplifier at various pump powers. (b) Output spectra of the second Tm:Tb:ZBLAN preamplifier at several pump powers. (c) Power spectra and (d) slope efficiency of the final power amplifier at different pump powers. The ASE spectrum of the Tm:Tb:ZBLAN fiber at 9.75 W is also shown in (c) alongside the amplified spectrum.

3. Pulse compression results

Previously, we used a fiber for pulse stretching [19]. This is not ideal because the introduced dispersion is already fixed and cannot be tuned once it is fabricated. We also utilized a grating-prism pair before where it is possible to compensate for the higher order of dispersion [20]. However, the added degrees of freedom, i.e., the distance between the grating and prism, complicates the optimization of the compression system. The current trend is the use of a CFBG which introduces a controlled amount of chromatic dispersion to an incident pulse [21]. Here, we report the use of a CFBG and a grating pair in tandem as well as dispersion matching between these elements. We use grating pairs only for pulse compression which is the standard for chirped pulse amplification (CPA) system [22]. The manufactured transmission gratings (*Gitterwerk*) in our system are capable of delivering extremely high diffraction efficiency ($\geq 97\%$).

The dispersion of our CFBG is determined by taking into account the complete group delay response of the grating compressor and total GDD of the amplifier system. The silica fibers of the fiber coupled devices (AOM, WDM, etc. in total 10 m of SMF28) contribute $\sim -0.5\text{ ps}^2$ whereas the ZBLAN fiber (1.6 m, 3.0 m and 4.0 m of Tm:Tb:ZBLAN) contributes insignificantly to the net dispersion that we do not take into account. The theoretically specified distance between the gratings in the Treacy compressor is 214 mm, the groove number of the gratings is 800 mm^{-1} and the incidence angle of the grating (Littrow angle) is 44.4° . Theoretically, the gratings

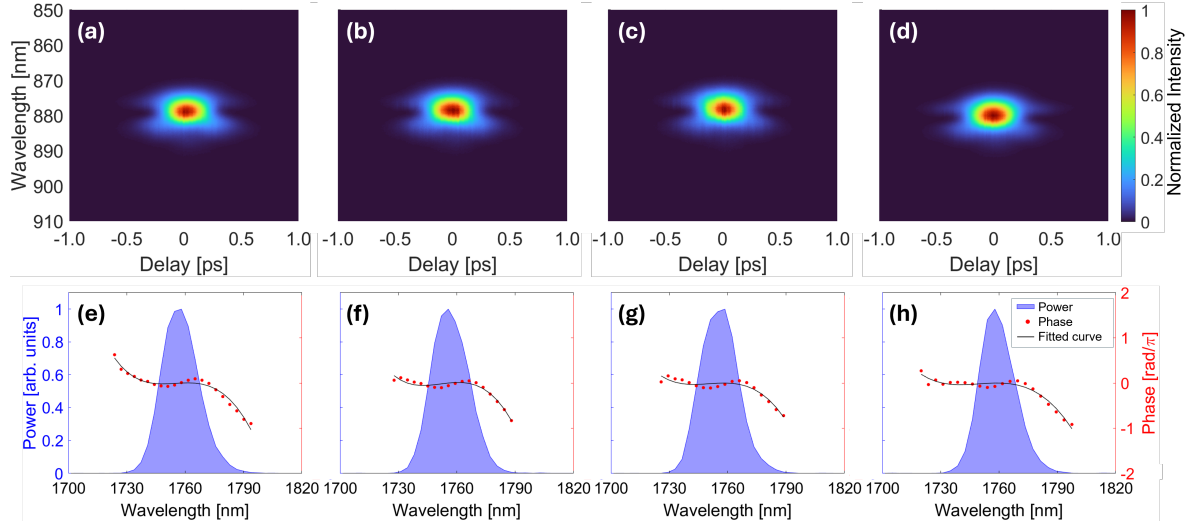


Figure 4. Normalized SHG-FROG traces (top row) of the output pulses from the power amplifier, with their corresponding retrieved spectral profile and phases (bottom row), for pump powers of (a,e) 2.23 W, (b,f) 5.10 W, (c,g) 9.13 W, and (d,h) 9.75 W.

introduce -7.15 ps^2 of second-order dispersion for a $1.75\text{ }\mu\text{m}$ incident beam. Based on these parameters, the designed dispersion of our CFBG is $+7.1435\text{ ps}^2$ and -0.0585 ps^3 for GDD and TOD, respectively. The TPSR implements a CFBG to achieve large dispersive pulse stretching within a compact fiber length.

At first, we investigated the effect of different pumping powers to the pulse duration of the retrieved spectrum for the case when the CFBG is not yet-fine tuned. We only adjusted the grating pair distance to obtain the shortest pulse duration and to minimize the GDD. The output of the grating pair is characterized using second harmonic generation frequency-resolved optical gating (SHG-FROG, *FemtoEasy*). The results are shown in Fig. 4. The optimal distance between the gratings was found to be 174 mm and was constant for all pumping powers. No significant difference on the measured pulse duration for different pump powers. The duration of the compressed pulse for 2.23 W, 5.10 W, 9.13 W, and 9.75 W were 220 fs, 220 fs, 227 fs, and 225 fs, respectively. From each retrieved spectral phase, we calculated the TOD at each pump power and determined that the absolute dispersion between 2.23 W and 9.75 W is sufficiently small ($\sim 10^{-5}\text{ ps}^3$). Hence, no evident phase distortion or nonlinear effects were observed in the SHG signal. Specifically, for a pump power of 9.75 W, as shown in Fig. 4(d,h), we compressed the pulse to 225 fs which is very close to its transform limited duration of 224 fs. Though we have not fine-tuned the CFBG, the pulse duration is already shorter than that of our previous system (254 fs) [19]. Moreover, the retrieved spectrum has a very low intensity in the $\geq 1.8\text{ }\mu\text{m}$ region compared to Ref. [4]. This means that we have mostly suppressed the ASE and that the output power of the compressed pulse came purely from the coherent part of the amplified pulse. That is also confirmed by a small residual phase within $\pm 0.5\pi$ retrieved from SHG-FROG.

Finally, we examine the tuning effect of the CFBG using a constant pumping power

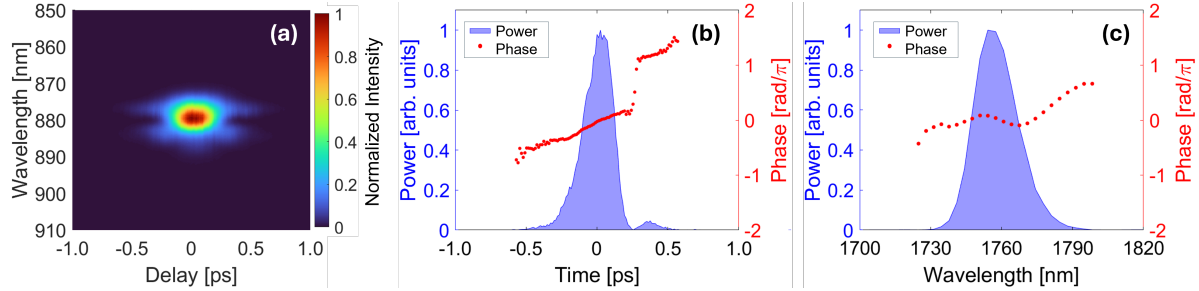


Figure 5. Pulse characterization result at a pump power of 9.75 W with CFBG fine-tuning. (a) The SHG-FROG trace of the compressed pulse by the grating pair. Retrieved pulse in (b) time and (c) frequency domain.

of 9.75 W and fix grating distance (174 mm). The FROG trace of the compressed pulse is shown in Fig. 5(a). The intensity and phase of the retrieved pulse in time and frequency domains are also shown in Fig. 5(b) and Fig. 5(c), respectively. Using an offset in the dispersion slope of -50 ps/nm^2 which corresponds to $\text{GDD}=7.1296\text{ ps}^2$ and $\text{TOD}=-0.0578\text{ ps}^3$, we measured the shortest pulse of 217 fs. The transform-limited pulse duration derived from the spectrum was 216 fs. The close match between the transform-limited and retrieved pulse duration proves that the CFBG dispersion profile was successfully compensated to that of the grating pair. Although some residual TOD can be seen in the spectral phase, we did not observe any serious phase distortion due to the nonlinear effects in the power amplifier. The compressed pulses peaked near $1.76\text{ }\mu\text{m}$, which is blue-shifted relative to our previous system [19]. Excellent temporal quality of the compressed pulse was also achieved as the retrieved temporal profile shows high contrast. That no considerable energy is distributed on the sides of the central pulse. Therefore, we expect that multi-photon excitation now will be more efficient. The power of the pulse after the Treacy compressor was estimated to be 700 mW.

4. Summary and conclusion

In summary, we have improved our previous CPA system by redesigning the amplification stage and incorporating a CFBG for tunable dispersion control in the compression stage. The output power reached $\sim 1\text{ W}$. With the controllable CFBG, we were able to compress the pulse to 217 fs. The pulse was compressed with reasonable spectral quality, as the spectrogram showed independence from the pumping power, and with an improved temporal profile, as it is free from side artifacts and strong nonlinear effects. We believe this is the first all-Tm:Tb:ZBLAN amplifier system that directly generates watt-level, short-wavelength ultrafast pulses. The construction of the all-Tm:Tb:ZBLAN amplifier system offers a simpler design while still delivering high average power and pulse duration near 200 fs, making it a suitable light source for three-photon lifetime imaging microscopy experiments with red fluorescent proteins [23–25].

Funding

National Institute for Physiological Sciences (24NIPS225, 25NIPS233); National Institute of Natural Sciences (OML0123008, OML012410);

References

- [1] Horton N G, Wang K, Kobat D, Clark C G, Wise F W, Schaffer C B and Xu C 2013 *Nature photonics* **7** 205–209
- [2] Wang M, Wu C, Sinefeld D, Li B, Xia F and Xu C 2018 *Biomedical optics express* **9** 3534–3543
- [3] Nomura Y, Murakoshi H and Fuji T 2020 *OSA Continuum* **3** 1428–1435
- [4] Murakoshi H, Ueda H H, Goto R, Hamada K, Nagasawa Y and Fuji T 2022 *Biomedical Optics Express* **14** 326–334
- [5] Sakamoto T, Shimizu M, Yamada M, Kanamori T, Ohishi Y, Terunuma Y and Sudo S 1996 *IEEE Photonics Technology Letters* **8** 349–351
- [6] Yamada M, Senda K, Tanaka T, Maeda Y, Aozasa S, Ono H, Ota K, Koyama O and Ono J 2013 *Electronics letters* **49** 1287–1288
- [7] Xu C, Nedergaard M, Fowell D J, Friedl P and Ji N 2024 *Cell* **187** 4458–4487
- [8] Guesmi K, Abdeladim L, Tozer S, Mahou P, Kumamoto T, Jurkus K, Rigaud P, Loulier K, Dray N, Georges P *et al.* 2018 *Light: Science & Applications* **7** 12
- [9] Khegai A, Melkumov M, Riumkin K, Khopin V, Firstov S and Dianov E 2018 *Optics letters* **43** 1127–1130
- [10] Nomura Y and Fuji T 2016 *Applied Physics Express* **10** 012703
- [11] Zhang J, Fu S, Sheng Q, Zhang L, Shi W and Yao J 2023 *Optics & Laser Technology* **158** 108882
- [12] Emami S D, Dashtabi M M, Lee H J, Arabanian A S and Rashid H A A 2017 *Scientific reports* **7** 12747
- [13] Chen S, Chen Y, Liu K, Sidharthan R, Li H, Chang C J, Wang Q J, Tang D and Yoo S 2021 *Optics letters* **46** 3637–3640
- [14] Chen J X, Zhan Z Y, Li C, Liu M, Luo A P, Zhou P, Xu W C and Luo Z C 2021 *Optics Letters* **46** 5922–5925
- [15] Chen S, Chen H, Sidharthan R, Chen Y, Tang D and Yoo S 2025 *Advanced Photonics Research* e202500068
- [16] Walsh B and Barnes N 2004 *Applied Physics B* **78** 325–333
- [17] Eichhorn M and Jackson S D 2008 *Applied Physics B* **90** 35–41
- [18] Krakowski M and Soboń G 2024 *Optics Express* **32** 48815–48823
- [19] Okada K, Banguilan D G, Ogawa K, Kajikawa E and Fuji T 2024 *Optics Continuum* **3** 1540–1547
- [20] Forget N, Crozatier V and Tournois P 2012 *Applied Physics B* **109** 121–125
- [21] Bartulevicius T, Frankinas S, Michailovas A, Vasilyeu R, Smirnov V, Trepanier F and Rusteika N 2017 *Optics express* **25** 19856–19862
- [22] Strickland D and Morou G 1985 *Opt. Comm* **56** 219
- [23] Cheng L C, Horton N G, Wang K, Chen S J and Xu C 2014 *Biomedical optics express* **5** 3427–3433
- [24] Liu H, Wang J, Peng X, Zhuang Z, Qiu P and Wang K 2018 *Journal of Biophotonics* **11** e201700351
- [25] Prevedel R, Ferrer Ortas J, Kerr J N, Waters J, Breckwoldt M O, Deneen B, Monje M, Soyka S J and Venkataramani V 2025 *Nature Reviews Neuroscience* 1–17